

THE CXFEL PROJECT AT ARIZONA STATE UNIVERSITY

W. S. Graves* on behalf of the CXFEL collaboration, Arizona State University, Tempe, AZ, USA

Abstract

The CXFEL is designed to produce attosecond-femtosecond pulses of soft x-rays in the range 250-2500 eV using nanobunched electron beams and a very high power laser undulator. The project includes 5 x-ray endstations with applications in biology, quantum materials, and AMO science. The CXFEL Project overall includes both the CXFEL and the nonlasing hard x-ray CXLS that is described elsewhere in these proceedings. The CXFEL has recently completed a 3-year design phase and received NSF funding in March 2023 for construction over the next 5 years. Both CXFEL and CXLS instruments use recently developed X-band distributed-coupling, room-temperature, standing-wave linacs and photoinjectors operating at 1 kHz repetition rates and 9300 MHz RF frequency. They rely on Yb-based lasers operating at high peak and average power to produce fs pulses of 1030 nm light at 1 kHz repetition rate with pulse energy up to 400 mJ. We present the design and initial construction activities of the large collaborative effort to develop the fully coherent CXFEL.

INTRODUCTION

Future light sources aim to improve performance, cost, and accessibility over today's instruments. The CXFEL project is developing femtosecond x-ray light sources at a cost and size that makes the novel time-resolved molecular science ultrafast light sources provide accessible to many institutions including universities, medical facilities, and industrial labs. The first instrument produced and now commissioning is the CXLS [1] that produces partially coherent synchrotron-like x-ray pulses at few hundred fs duration in the hard x-ray range. The second instrument, CXFEL, has completed design and is now under construction. It is a further development of CXLS technology that adds novel nanometer-scale electron bunching to produce fully coherent x-rays in the soft x-ray spectrum.

X-RAY SCIENCE DRIVERS

CXFEL is designed to address ultrafast dynamics in biochemistry, AMO science, and quantum materials. In the biological sciences it will map the energy landscapes of molecular machines and the conformational motions vital to their function. Other examples include the dynamics of the riboswitch that regulates protein production, ultrafast molecular processes involved in light-sensitive proteins, such as those involved in photosynthesis, and the chemistry of antibiotic resistance. Our AMO science effort aims to advance the understanding of fundamental light-matter interactions with implications for the mechanisms that underlie the chemistry of life, and to develop novel AI/ML-based data-analytical

Table 1: CXFEL Design Performance at several photon energies. Brilliance units are $\text{ph}/(\text{s} \cdot 0.1\% \cdot \text{mm}^2 \cdot \text{mrad}^2)$.

Photon energy (eV)	250	1000
Photons/pulse	8×10^8	1.1×10^8
Pulse rate (Hz)	1000	1000
Avg flux (ph/s)	8×10^{11}	1.1×10^{11}
Flux/shot (nJ)	32	18
Avg brilliance	1.3×10^{15}	1.2×10^{16}
Peak brilliance	1.2×10^{28}	5.6×10^{28}
Round RMS src size (μm)	0.9	0.5
Round RMS src angle (μrad)	440	188
FWHM pulse length (fs)	9.1	4.6
FWHM bandwidth (%)	0.18	0.09
Arrival timing jitter (fs)	< 10	< 10
Electron beam energy (MeV)	14	29

techniques. CXFEL will illuminate the role of attosecond electronic correlations and electron-nuclear couplings that drive femtosecond rearrangements of atoms, enabling better understanding and control of interfacial processes at the heart of emerging sunlight-to-fuel and sunlight-to-electricity concepts. CXFEL's tunable attosecond pulses can reveal the nature of driven quantum matter, from non-thermal phase transitions to strongly-driven coherent states, and access key dynamic processes relevant for advanced functional materials with photovoltaic, magnetic storage, and information processing applications.

CXFEL INSTRUMENT

The CXFEL design parameters are shown in Table 1 and the layout of the source is shown in Fig. 1. CXFEL is a further development of the technologies used in CXLS that is designed to produce fully coherent x-ray pulses. The accelerator components are nearly identical to CXLS with the addition of an electron diffraction [2] chamber and emittance exchange (EEX) [3] line. The components also apply lessons learned with CXLS to improve performance. The purpose of the additional equipment is to create nanobunches of electrons that are short on the x-ray wavelength scale, i.e. < 1 nm in length so that when they interact with the ICS laser the output is coherent. Our initial effort is focused on generating coherent radiation in the soft x-ray energy range of 250–1000 eV with a stretch goal to reach 2.5 keV. The method of creating nanobunches is sensitive to power supply jitter in the magnets and RF cavities that comprise the EEX line. Current state-of-the-art equipment performance is at the level of 50 parts per million (PPM) stability which is good enough to produce soft x-ray radiation. In future phases we hope to extend the energy range to 10 keV for crystallography studies which will require equipment stability below 10 PPM. The steps to produce the nanobunched

* wsg@asu.edu

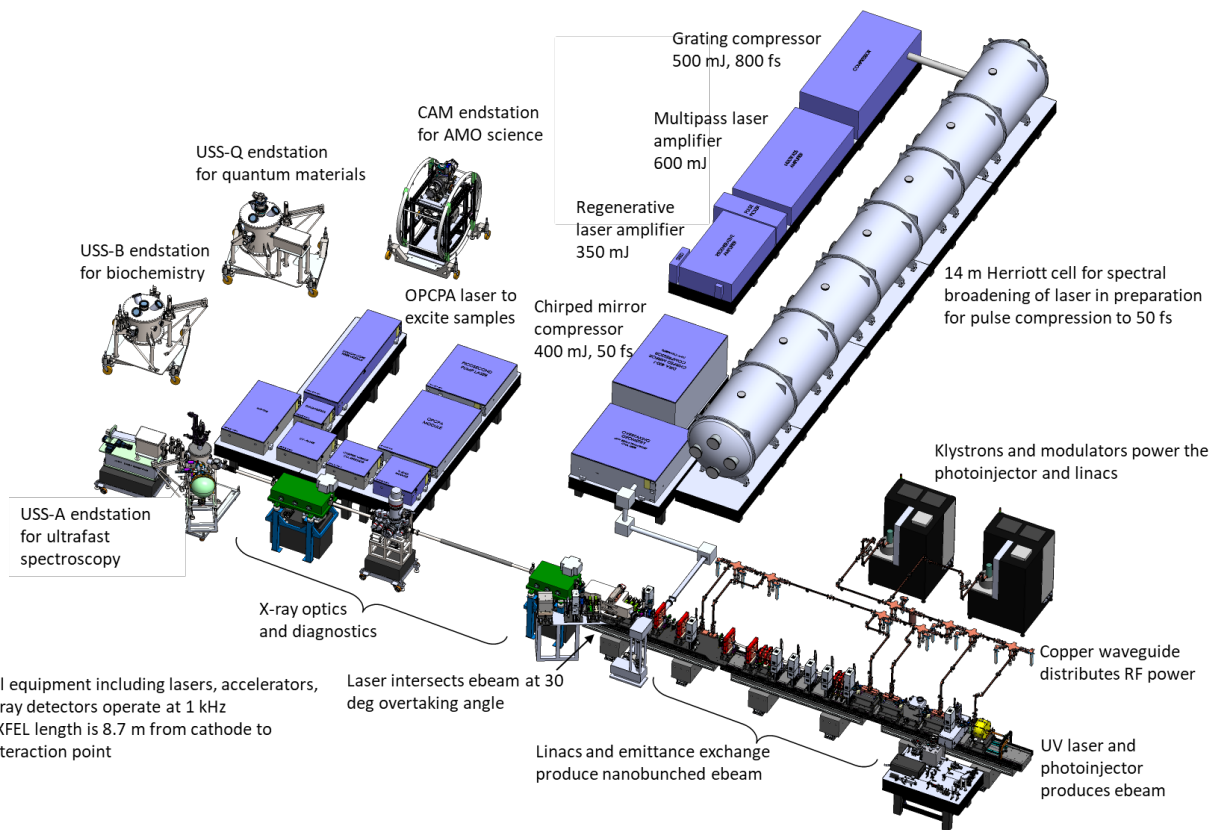


Figure 1: Major components of CXFEL including ICS laser at center top, RF and accelerator at lower right. Electron beam travels from right to left. X-ray beamline, sample pump laser and x-ray endstations are at left. Each of the endstations shown are installed for different experiments. The source length from cathode to laser interaction point is 9 m.

beam include acceleration in the photoinjector and first linac section L1 to an energy of 9 MeV, then diffraction on lithographically patterned Si gratings with period ranging from 50–500 nm. Diffraction through the grating generates two populations of electrons, one of which is diffracted and collimated away and the other continues to propagate straight ahead. The stripes in the beam shear in transverse phase space within a few cm, washing out the purely spatial modulation but retaining distinct modulations within 2D phase space. This shearing prevents local space charge debunching since the beam is again spatially uniform. After diffraction the beam is accelerated to final energy and then demagnified in the EEX matching section. The EEX line then converts the transverse 2D modulation to a 2D longitudinal modulation containing highly correlated nanobunches in time and energy. At the EEX exit the phase space orientation of the nanobunches are in a "focusing" orientation. They then propagate to the interaction point where the nanobunches reach a waist in longitudinal space providing the needed modulation at x-ray wavelength.

Producing x-rays in this lower energy range is not well suited to the head-on collision geometry commonly used for ICS x-ray production where the effective undulator period is just 515 nm for a 1030 nm ICS laser. Such a short undulator period requires an ebeam energy in the few MeV range to make soft x-rays. Such low energy electrons are subject to

strong space-charge forces and difficult to focus to a small interaction spot. Instead we adopt an "overtaking" collision geometry where the electron beam and laser propagate in the same direction with a 30° angle between them resulting in an effective undulator period of 8 μm thus raising the ebeam energy to e.g. 29 MeV to produce 1 keV photons. This geometry does however require a substantially more powerful and shorter pulse ICS laser as discussed below.

Accelerator and RF Systems

The low-level RF (LLRF) system is a hybrid analog-digital system based on IQ modulation/demodulation (IQM/IQD) developed at ASU. We are building on the CXLS LLRF system that is based on National Instruments PXIe chassis and 14-bit ADC cards. We are integrating the IQD and digitizer circuits from separate components into a custom PXIe FPGA front end card with 18-bit digitizer chips to improve performance. The IQM circuits drive 100 W solid-state power amplifiers that in turn drive a pair of Stellant L-6145 klystrons to 6 MW output. Scanditronix K200 solid-state modulators have been customized with additional charging power supplies with the goal of providing 10 PPM stability of the klystron output while pulsing at 1000 pulses per second. The modulator trigger circuits are also upgraded to improve timing by an order of magnitude. From studies with CXLS we have learned that having a single RF source drive multi-

ple accelerator sections produces correlated jitter in phase and amplitude that can be used to reduce the overall electron beam timing and energy jitter by properly phasing the accelerator sections using our high power Variable Phase Shifter Power Dividers (VPSPDs) developed at SLAC. The VPSPDs are waveguide structures that can combine or split RF power controlling both the phase and power division at the 2 outputs. We use one VPSPD to combine power from both klystrons into a single 2 microsecond, 12 MW pulse. This pulse is then compressed with a compact SLED compressor [4] to 200 ns, 40 MW power and distributed among the photoinjector, linac sections, and EEX RF deflector by multiple VPSPDs as shown in Fig. 1. Any fluctuations in phase and amplitude are 100 % correlated among the various accelerator sections allowing the electron beam timing and energy jitter to be greatly reduced by proper phasing of the sections.

The accelerator consists of a 4.5 cell photoinjector and three 35-cm linac sections of 20 cells each as shown in Fig. 1. All of the accelerator structures are high efficiency 9.3 GHz standing-wave room-temperature copper structures with a repetition rate of 1 kHz and fill time of 150 ns. The photoinjector is a further development of the CXLS photoinjector [5] with improved cathode cooling and an extended entrance beampipe to allow for the larger solenoid magnet required for this higher energy device. The design peak cathode field is 150 MV/m and exit energy is 5 MeV for 4 MW input power. The solenoid magnet again uses tape-wound, edge-cooled coils that have proven very successful in CXLS. Compared with CXLS the new solenoid has smaller bore, redesigned iron nose cones to lower the longitudinal B-field gradient at the cathode, longer overall length, and higher excitation for this higher gradient injector.

The linacs are innovative distributed-coupling structures [6] with a high shunt impedance of 150 MΩ/m. The cell geometry is modified from CXLS to produce a lower ratio of surface E-field to gradient (2:1) instead of the 4:1 ratio of CXLS. This lowers the shunt impedance and efficiency slightly while permitting higher gradient operation. We plan to operate the new design at gradient up to 75 MV/m requiring 12 MW per linac for 24 MeV energy gain per linac. The beam energy is 5 MeV entering linac L1 which is at relatively low gradient to limit beam energy below 10 MeV at the electron diffraction location between L1 and L2. L2 and L3 then accelerate to final energy up to 60 MeV needed to produce 2.5 keV photons. Most operations will be at lower beam energy to generate photons in energy range 0.25–1 keV.

Lasers and Timing Systems

The photocathode laser is a LightConversion Pharos Yb:KGW amplifier producing 2 mJ pulses of 1030 nm light with FWHM 150 fs at 1 kHz repetition rate. The single-box laser has a 4th harmonic module that produces up to 100 μJ of 258 nm light that produces the electron beam at the photocathode. CXFEL requires a very low emittance less than

50 nm·rad, thus the laser is focused to a small spot on the cathode and total charge generated is 1-2 pC per pulse.

The ICS laser begins with a 350 mJ Yb:YAG thin-disk regenerative amplifier followed by a 600 mJ multipass amplifier and grating compressor to 800 fs pulses at 1 kHz repetition rate all supplied by Trumpf Scientific Lasers. The overtaking geometry used by CXFEL requires short high energy pulses with tilted pulse fronts to produce an effective laser-electron interaction length up to 2 mm. ASU and Trumpf are jointly developing a large (14 m) gas-filled Herriott cell [7] to provide spectral broadening of the 600 mJ pulses enabling compression in a chirped mirror compressor to 50 fs or shorter.

The photoinjector and ICS lasers are synchronized to each other and to the RF system using balanced optical modulators (BOMPDs) from Cycle Laser in Hamburg. Expected timing error is approximately 10 fs. The ebeam timing jitter is compressed due to beam dynamics in the accelerator and EEX line and may approach 1 fs.

X-RAY PERFORMANCE AND CONSTRUCTION STATUS

Initial simulations [8] with the Mithra code [9] indicate output at approximately 10 MW peak power in pulse lengths ranging from 0.5–5 fs and other properties shown in Table 1 across a range of energies. We are in the process of exploring the impact of optimizations on start-to-end simulations on x-ray output power and stability with particular attention to the jitter requirements for key equipment.

Construction of the instrument commenced in March 2023 with first beam expected in 2027. Current construction activities include lab renovations to accommodate the large ICS laser and procurement of major equipment with long lead times.

ACKNOWLEDGMENTS

This work is supported by NSF Awards 2153503 and 1935994.

REFERENCES

- [1] W. Graves *et al.*, “Results from CXLS commissioning”, presented at IPAC’24, Nashville, TN, USA, May 2024, paper TUCN3, this conference.
- [2] L. Malin *et al.*, “Quantitative agreement between dynamical rocking curves in ultrafast electron diffraction for x-ray lasers”, *Ultramicroscopy*, vol. 223, p. 113211, 2021.
doi:10.1016/j.ultramic.2021.113211
- [3] E. A. Nanni, W. S. Graves, and D. E. Moncton, “Nanomodulated electron beams via electron diffraction and emittance exchange for coherent x-ray generation”, *Phys. Rev. Accel. Beams*, vol. 21, no. 1, p. 014401, 2018.
doi:10.1103/PhysRevAccelBeams.21.014401
- [4] M. Franz, J. Wang, V. Dolgashev, and S. Tantawi, “Compact rf polarizer and its application to pulse compression systems”, *Phys. Rev. Accel. Beams*, vol. 19, no. 6, p. 062002, 2016.
doi:10.1103/PhysRevAccelBeams.19.062002

[5] W. S. Graves *et al.*, “Design of an X-Band Photoinjector Operating at 1 kHz”, in *Proc. IPAC’17*, Copenhagen, Denmark, May 2017, pp. 1659–1662.
doi:10.18429/JACoW-IPAC2017-TUPAB139

[6] S. Tantawi, M. Nasr, Z. Li, C. Limborg, and P. Borchard, “Design and demonstration of a distributed-coupling linear accelerator structure”, *Phys. Rev. Accel. Beams*, vol. 23, no. 9, p. 092 001, 2020.
doi:10.1103/PhysRevAccelBeams.23.092001

[7] Y. Pfaff *et al.*, “Nonlinear pulse compression of a 200 mJ and 1 kW ultrafast thin-disk amplifier”, *Opt. Express*, vol. 31, no. 14, pp. 22 740–22 756, 2023.
doi:10.1364/OE.494359

[8] E. Ros, L. Malin, R. DeMott, S. Teitelbaum, S. Tilton, and W. Graves, “Simulation of CXFEL with MITHRA code”, presented at IPAC’24, Nashville, TN, USA, May 2024, paper MOPG13, this conference.

[9] A. Fallahi, A. Yahaghi, and F. X. Kärtner, “Mithra 1.0: A full-wave simulation tool for free electron lasers”, *Comput. Phys. Commun.*, vol. 228, pp. 192–208, 2018.
doi:<https://doi.org/10.1016/j.cpc.2018.03.011>